

Power-law exponent in the central region of a polymer layer adsorbed from dilute solution: comparison between scaling and SCF results

G.J. Fleer, F.A.M. Leermakers

Department of Physical and Colloid Chemistry, Wageningen Agricultural University,
Dreijenplein 6, 6703 HB Wageningen, The Netherlands

Abstract

De Gennes predicted the self-similar structure $\varphi(z) \propto z^{-\alpha}$ for adsorbed polymer layers in the semi-dilute (central) region of the adsorption profile of homopolymers. This power-law behaviour is recovered in mean-field SCF calculations. In this case the exponent is $\alpha = 2$ in good solvents provided $D \ll z \ll d$, where D is the proximal length and d the distal length. We use a ground-state approximation (GSA) to derive expressions for the two lengths D and d , and show that in the central region the profile is in good approximation given by $\varphi = \frac{1}{3}(z+D)^{-2} \exp\left(-(z+D)^2/3d^2\right)$. Unless the chains are extremely long the condition $D \ll z \ll d$ is difficult to obtain and corrections on the exponent are necessary. For most chain lengths in the experimental range, the central region is quite narrow. It is shown that for high adsorption energies (small D) $\alpha \approx 2 + 2d^{-1}$ in leading order, where $d \approx R/\sqrt{\ln(1/\varphi^b)}$, with R the radius of gyration and φ^b the bulk solution concentration. For weak adsorption the proximal length D is larger, which leads to a smaller exponent α . The d^{-1} correction is in excellent agreement with numerical self-consistent-field calculations. In poor solvents we have $\varphi = \frac{1}{2}(z+D)^{-1} \exp\left(-2(z+D)^2/3d^2\right)$ and $\alpha \approx 1 + 4d^{-1}$ in the strong adsorption limit, which implies a larger correction in this case. Our analysis suggests that in a polymer adsorption profile with excluded-volume correlations (where $\alpha = 4/3$) non-universal aspects would also be present if the chain length is finite.

Introduction

The influence of an impenetrable wall on the conformational properties of adsorbed homopolymers has been the subject of a large number of studies [1]. This interest is partly due to the many technological applications and partly because of the rich physical behaviour of such systems. In view of the many repeating units in the polymer chain universal aspects of the adsorption behaviour are anticipated. For example, even when the short range interactions with the surface are only of order kT per segment, the large number of chain segments causes an adsorption isotherm of the high-affinity type. The chain conformations on the surface are characterised by adsorbed trains and by loops and tails sticking out. It is remarkable that the overall density profile of such an adsorbed layer remains relatively simple. As shown by De Gennes [2], the layer splits up into a *proximal* region (characterised by a proximal length D), a *central* region ($D \ll z \ll d$, where d is the distal length) and a *distal* region ($z \gg d$). The distal region (where the profile decays

exponentially towards the bulk value) will not be treated in this paper in detail. Here we focus on the central part of the segment density profile.

Both experimentally and theoretically it is recognised that in semi-dilute polymer solutions the properties become essentially independent of the chain length N . In good solvents and for concentrations above $\phi^* \propto N^{-4/5}$, the characteristic mesh (or blob) size ξ depends only on the segment concentration ϕ^b : $\xi \propto (\phi^b)^{-3/4}$. On length scales smaller than ξ , the (sub)chains behave as self-avoiding walks and are thus swollen. On length scales larger than ξ , the excluded-volume correlations are screened. Thus the chains split up into a necklace of blobs, the size of which decreases with increasing ϕ^b . At a concentration ϕ^{**} there is a cross-over from the semi-dilute to the concentrated regime. In this concentrated regime all excluded-volume interactions are screened and the chains behave ideally, i.e., mean-field-like: $\xi \propto (\phi^b)^{-1/2}$.

These solution features must play a role as well in an adsorbed layer. In the semi-dilute part of the adsorption profile, the polymer segment density drops from a high value near the surface to a lower value away from it. The characteristics of this decay can be found from a scaling argument. At a position z from the surface the density cannot be lower than $z^{-4/3}$ because if this would happen the local mesh (blob) size would exceed the distance to the wall. In other words, the blob would not fit in. As the width of density gradients in interfacial systems tends to be minimized, we thus expect that the profile will drop as quickly as possible, i.e., according to $\phi(z) \propto z^{-4/3}$. This scaling argument should apply within the semi-dilute part of the profile, for densities $\phi(z)$ in excess of ϕ^* but below ϕ^{**} .

Closer to the surface the concentrations are high, approaching unity for relatively high adsorption energies, and we expect a mean-field scaling $\phi(z) \propto z^{-2}$ over a narrow region. At some distance near the surface (at the point where $\phi(z) = \phi^{**}$) the profile crosses from this concentrated region ($\phi(z) \propto z^{-2}$) towards the semi-dilute regime ($\phi(z) \propto z^{-4/3}$). At low adsorption energies χ_s the density near the surface might not enter the concentrated region and the profile could follow the scaling according to $\phi(z) \propto z^{-4/3}$ all the way from D to d . In order to obtain a well-defined central region we should have the condition that $D \ll d$. In the scaling theory d is supposed to scale as the radius of gyration R , which in good solvents is proportional to $N^{3/5}$.

In a mean-field theory the scaling in the concentrated and dilute regimes is the same, i.e., $\xi \propto (\phi^b)^{-1/2}$, and thus in a mean-field picture the self-similar profile would be expected to span the whole region between the proximal length D (which turns out to be smaller than the segment size for high χ_s) and the distal length d . If d would be equal to R (where now $R \propto N^{1/2}$), there might still be a wide central region with $\phi(z) \propto z^{-2}$. However, as we shall see below, d is considerably smaller than R , by a factor $\sqrt{\ln(1/\phi^b)}$, which narrows the central region.

The effects of finite chain length and solution concentration on the central part of the profile can possibly best be illustrated in a mean-field framework. This might be true for the following reasons: (i) In a mean-field adsorption profile we expect no problems when crossing from the concentrated to the semi-dilute parts of

the profile. Therefore we can easily study the strong adsorption limit. (ii) The mean-field theory can be enumerated exactly up to chain lengths of order 10^6 , and analytically with a few approximations.

A few years ago, Van der Linden and Leermakers [3] analysed the profiles computed with the self-consistent-field theory of Scheutjens and Fleer [1,4,5] for very long chains and a relatively high adsorption energy ($\chi_s = 1$). From the above it is clear that one should expect the central part of the profile to be self-similar with the mean-field power law $\phi(z) \propto z^{-2}$. Indeed, this was found for chain lengths of order 10^5 and above, corresponding to molar masses of several millions or even higher. For smaller (but still very long) chains they found a correction which was a function of the chain length and the volume fraction of polymer in the bulk solution. Such a correction would imply a non-universal behaviour in the central region of the profile. Although we now believe that Van der Linden and Leermakers overestimated the correction somewhat, it is still worth while to interpret this type of data, especially since better analytical approximations have become available [6-9]. We note that in an adsorbed layer adsorbed from semi-dilute solutions such chain-length dependent corrections do not play a role; in that case the relevant length scale is the correlation length in the bulk of the solution, which does not depend on N .

In this paper we undertake an attempt to analyse the dilute case with a simple analytical model. The starting point is the well-known ground-state approximation (GSA). In this approach the ranking number dependence of the density profile is lost, which implies that tail segments have the same distribution as loop segments in the overall density profile. We know that this is wrong, especially in the distal part of the profile, which decays to the bulk a factor of two too fast in a GSA approximation. Recently, Johner et al. [7] elaborated an elegant method to include the effect of tails. Earlier, Scheutjens et al. [10] had tried this in a more primitive and partly intuitive way. Here we are interested mainly in the proximal and central regions of the profile where tails contribute only slightly, so that the simpler GSA approximation is still adequate.

The self-similar density profile in mean-field GSA

The partition function for a polymer-solvent system near a surface can be written as a functional integral over all possible trajectories of the polymer chains. As shown by Hong and Noorlandi [11] the mean-field approximation is found by taking the maximum of the integrand with the constraint of local incompressibility of the polymer-solvent mixture. The result of this procedure is a modified diffusion equation for the end-point distribution function $G(r,s)$ of a polymer fragment of length s with one end ($s' = 1$) unrestricted in space and the other end ($s' = s$) fixed at a coordinate r . This diffusion equation was first introduced by Edwards [12]. It is easily shown [1,6] that, when the density gradients are small, this continuum differential equation is the same as the discretised propagator (recurrence) relation used in the Scheutjens-Fleer formalism [1]. We expect the system to remain homogeneous parallel to a wall. This allows us to treat it as a one-dimensional problem with a z -coordinate perpendicular to the interface, which is positioned at $z = 0$:

$$\frac{\partial G}{\partial s} + uG = \frac{1}{6} \frac{\partial^2 G}{\partial z^2} \quad (1a)$$

This equation is valid when G is a slowly varying function of z and s . In that case it is equivalent to the lattice SCF equation

$$G(z, s+1)e^{u(z)} - G(z, s) = \frac{1}{6} \{G(z-1, s) - 2G(z, s) + G(z+1, s)\} \quad (1b)$$

In these expressions, $G = G(z, s)$ is an end-point distribution function for a chain fragment of s segments long which ends at a distance z from the surface, and $u(z)$ is the segment potential which varies perpendicular to the wall in a way to be specified below. The continuum equation 1a has the advantage that it can provide analytical solutions, which is very difficult with the discrete version 1b; however, the latter is also applicable when u is high and for steep gradients in G .

In order to obtain such analytical solutions from eq. 1a, further approximations are necessary. The standard ground-state approximation (GSA) is to write $G(z, s)$ as the product of a ground-state eigenfunction $g(z)$ and the s -th power of the largest (= ground-state) eigenvalue e^ϵ :

$$G(z, s) = g(z)e^{\epsilon s} \quad (2)$$

The implication of this approximation is the loss of the ranking number dependence in the density profile; each segment along the chain contributes equally to the density profile irrespective whether it is an end segment or an interior segment. Concentrating on the interior segments, we realise that the volume fraction profile $\phi(z, s)$ due to segment s is proportional to $G(z, s)G(z, N-s)$ because the two walks $1, 2, \dots, s$ and $N, N-1, \dots, s$ both should end in z . The segment density profile is now found by

$$\phi(z) = \phi^b e^{\epsilon N} g^2(z) \quad (3)$$

Quite often the approximation $\phi^b e^{\epsilon N} = 1$ is made. Although it can be shown that this approximation can be avoided, it will suffice for the moment. Then ϵ is defined by

$$\epsilon = \frac{1}{N} \ln \left(\frac{1}{\phi^b} \right) \quad (4)$$

Upon substitution of eq. 2 into eq. 1a the ground-state differential equation in $g(z)$ is obtained:

$$\frac{1}{6} \frac{d^2 g}{dz^2} = (u + \epsilon)g \quad (5)$$

which may be solved if $u = u(z)$ can be expressed in $g(z)$. In good solvents it is known that $u(z) = -\ln[1 - \phi(z)] = \phi(z)$, which is basically a Flory-Huggins expression, also used by De Gennes. Hence,

$$u(z) = \varphi(z) = g^2(z) \quad (6)$$

The GSA equation now takes the well-known form:

$$\frac{1}{6} \frac{d^2 g}{dz^2} = (g^2 + \epsilon) g \quad (7)$$

and has the solution [6-9]:

$$g = \sqrt{2\epsilon} \operatorname{csch}[(z+D)\sqrt{6\epsilon}] \quad (8)$$

where $\operatorname{csch} x = 1/\sinh x$. The integration constant D has to be found from the boundary condition at the surface. It is easily verified that D equals $D = -g(0)/(dg/dz)_0$, so that D can also be considered as the extrapolation length. Because $\operatorname{csch} x = 2e^{-x}$ for large x , we conclude that $\sqrt{6\epsilon}$ serves as the reciprocal exponential decay length far from the surface. Hence we define $d \equiv 1/\sqrt{6\epsilon}$. With eq. 4 we have

$$d = \frac{\sqrt{N/6}}{\sqrt{\ln(1/\varphi^b)}} = \frac{R}{\sqrt{\ln(1/\varphi^b)}} \quad (9)$$

where $R = \sqrt{N/6}$ is the radius of gyration of ideal chains. In terms of d we can write the density profile $\varphi = g^2$ as:

$$\varphi = \frac{1}{3d^2} \operatorname{csch}^2\left(\frac{z+D}{d}\right) \quad (10)$$

It is of some interest to consider the limiting behaviour of the density profile for small $1/d$. Then we may expand $\ln \varphi$ (eq. 10) and $\ln g$ (eq. 8) in terms of $1/d$. The result is:

$$g = \frac{1}{\sqrt{3(z+D)}} \exp\left(-\frac{(z+D)^2}{6d^2}\right) \quad \varphi = \frac{1}{3(z+D)^2} \exp\left(-\frac{(z+D)^2}{3d^2}\right) \quad (11a,b)$$

We will show below that eq. 11 is remarkably good upto the dilute part of the density profile. For $D \ll z \ll d$, eq. 11b reduces to the simple scaling law $\varphi(z) \propto z^{-2}$ discussed above.

The next step is to find an expression for the parameter D as a function of the adsorption energy χ_s . This is a tricky problem since it involves the boundary condition at the surface. On the length scale of the segment size or below, the continuum description (eq. 1a) is expected to break down and the discretised version (eq. 1b) is more appropriate. We try to connect the continuum approach to a lattice model. In lattice models, the layers are numbered $z' = 1, 2, \dots$, where the layer number z' is an integer. Adsorbed segments are in the first (or surface) layer ($z' = 1$). In a continuum model with the wall at $z = 0$ it is logical that the centre of adsorbed segments would be at $z = 1/2$. We therefore identify $\varphi(z')$ in the lattice model with $\varphi(z)$ in the

continuum description, where $z = z' - 1/2$. This procedure is illustrated in fig. 1. In terms of z , the layers are at coordinates $z = 1/2, 3/2, \dots$.

Consequently, we determine D by substituting eq. 2 into eq. 1b for $z = 1/2$, which gives:

$$g(\frac{1}{2})e^{\epsilon+u(\frac{1}{2})} = \frac{1}{6} \left[4g(\frac{1}{2}) + g(\frac{3}{2}) \right] \quad (12)$$

where $g(-1/2) = 0$ because layer $z' = 0$ is in the adsorbent and thus forbidden for polymer segments.

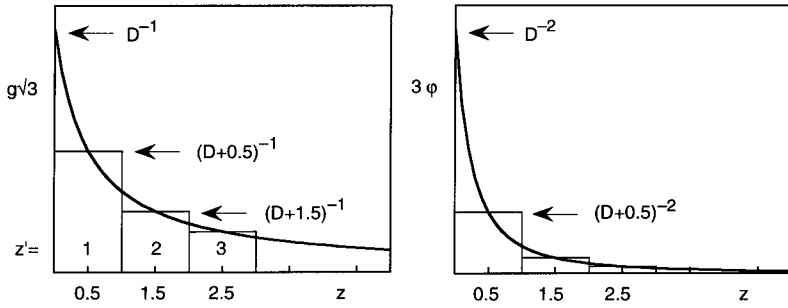


Fig. 1. Illustration of the mapping of continuum and lattice models. The centre of the lattice layers is at $z = 1/2, 3/2, \dots$.

For the conditions relevant in the present paper ϵ may be neglected with respect to $u(1/2)$, the field experienced by adsorbed segments. For these segments, the volume fraction may be high so that the approximation $-\ln(1-\phi) = \phi$ no longer holds. We should use the full Flory-Huggins expression, which basically corresponds to the excluded volume condition: the term $1-\phi$ is the solvent volume fraction and originates from the constraint that the volume fractions of polymer and solvent should add up to unity. In addition, the adsorption energy χ_s comes in. Hence $u(1/2) = -\ln[1-\phi(1/2)] - \chi_s$, which is the same as in the Scheutjens-Fleer model [1,4,5]. According to equation 11b we have $\phi(1/2) = (1/3)(D+1/2)^{-2}$. Substituting $e^{-u(1/2)} = [1-\phi(1/2)]e^{\chi_s}$ and $g(3/2)/g(1/2) = (D+1/2)/(D+3/2)$ (eq. 11a) into eq. 12 we find an equation that contains D as the only unknown:

$$\left(1 - \frac{1}{3(D+1/2)^2} \right) \left(4 + \frac{D+1/2}{D+3/2} \right) = 6e^{-\chi_s} \quad (13)$$

This equation could be rearranged to give a cubic equation in the parameter $x \equiv (D+1/2)^{-1}$, which could be solved explicitly; since the outcome is a cumbersome expression we will not do that here. The solution of

eq. 13 is plotted in fig 2 (solid curve). The proximal length D is large for χ_s close to $\chi_{sc} \equiv \ln(6/5)$, and it decreases until at high χ_s a constant level $D = 0.077$ is reached.

For small $\chi_s - \chi_{sc}$ the first factor $1 - \varphi(1/2)$ in eq. 13 is nearly unity (i.e., the excluded volume does not yet play an important role). The second factor is then approximately equal to $6e^{-\chi_s} = 5e^{\chi_{sc} - \chi_s}$, which is close to 5; hence $(D+1/2)/(D+3/2)$ is nearly unity and D is large. Expanding the left-hand side of eq. 13 in terms of $x = (D+1/2)^{-1}$ up to second order, we obtain the equation $2x^2 + 3x = 18(e^{-\chi_{sc}} - e^{-\chi_s})$. The solution for D is

$$D = \frac{4/3}{-1 + \sqrt{1 + 16(e^{-\chi_{sc}} - e^{-\chi_s})}} - \frac{1}{2} \quad (14)$$

This dependence is given in fig. 2 as the dotted curve; it is accurate only for $\chi_s - \chi_{sc} < 0.1$. For even smaller χ_s eq. 14 reduces to the asymptotic limit $D = \frac{1}{6}(\chi_{sc} - \chi_s)^{-1} - \frac{1}{2}$, valid for $\chi_s - \chi_{sc} < 0.04$. The scaling behaviour $D \propto (\chi_s - \chi_{sc})^{-1}$ for undersaturated layers has been derived before [1,7].

As the surface becomes more occupied for higher χ_s the factor $1 - \varphi(1/2)$ in eq. 13 is no longer unity. At very high χ_s , $\varphi(1/2) \approx 1$ and $3(D+1/2)^2 = 1$, or $D = 1/\sqrt{3} - \frac{1}{2} = 0.077$. For this value of D , the second factor in eq. 13 is $4 + 0.366$, and eq. 13 reads $1 - \varphi(1/2) = 1.37e^{-\chi_s}$. Replacing the numerical factor 3×1.37 by 4, we get the strong adsorption limit for D as

$$D = \frac{1}{\sqrt{3 - 4e^{-\chi_s}}} - \frac{1}{2} \quad (15)$$

which relation holds rather accurately for $\chi_s > 0.5$, as shown by the dashed curve in fig. 2.

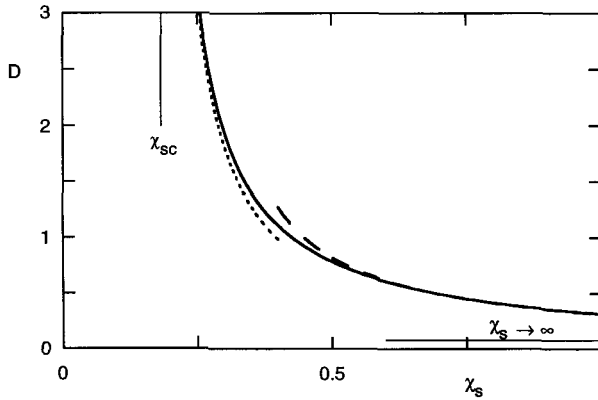


Fig. 2. The dependence $D(\chi_s)$ according to eq. 13 (solid curve). The asymptotic relations for small $\chi_s - \chi_{sc}$ (eq. 14, dotted) and for high χ_s (eq. 15, dashed) are also indicated.

Volume fraction profiles

An example of volume fraction profiles obtained from the numerical SCF model and calculated from the GSA equations is given in fig. 3. This figure applies to $N = 10^4$, $\varphi^b = 10^{-7}$, and $\chi_s = 1$ and gives $\log[\varphi(z)]$ as a function of $\log(z)$, where $z = z' - 1/2$ as discussed above. The GSA curves were calculated for $D = 0.313$ (from eq. 13 or 15) and $d = 10.75$. The latter value is slightly higher than that found from eq. 9 ($d_0 = 10.17$) as it was computed from a better approximation:

$$\left(\frac{d_0}{d}\right)^2 = 1 + 2 \frac{\ln f}{\ln(1/\varphi^b)} \quad f \approx \frac{1}{\sqrt{3}} \frac{1/D - 1/d_0}{\ln(2d_0/D)} \quad (16a,b)$$

where d_0 is the value of d as obtained from eq. 9. The derivation of eq. 16 will be given elsewhere; it is based upon the constraint that end segments and middle segments should have the same abundance in the system, which can be translated into the condition $\int g dz = \int g^2 dz$. The implication is that the factor f in eq. 16b, which is defined by $f^2 = \varphi^b e^{\varepsilon N} = \varphi^b \exp(N/6d^2)$ is no longer unity, as was assumed in eq. 4.

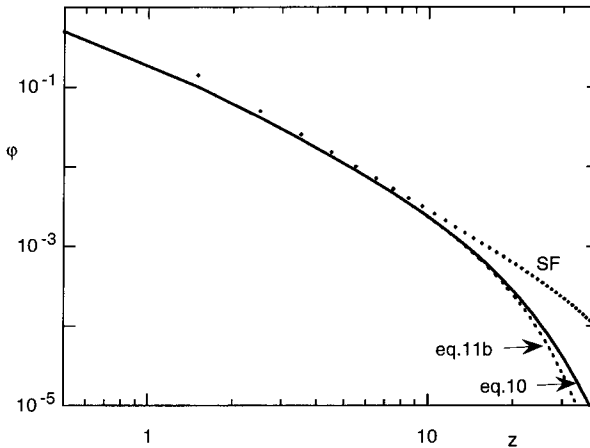


Fig. 3. Double-logarithmic plot $\varphi(z)$ according to the numerical results (data points) and in GSA (eqs. 10 and 11b), for $N = 10^4$, $\varphi^b = 10^{-7}$, and $\chi_s = 1$. The GSA curves were calculated with $D = 0.313$ and $d = 10.75$.

In fig. 3 the GSA prediction (solid curve) corresponds to the full expression 10, the dotted curve was obtained from the simplified equation 11b. It is clear that the latter equation is fully adequate up to well beyond $z = d$, i.e., over the entire central region. The deviation occurring in the distal regime is of no concern for our present purpose.

Comparing the GSA results with the numerical data we see excellent agreement in the surface layer (the difference here is well below 1%) and over most of the central region, where GSA is only a few % lower than SF. As expected, for $z \gg d$ the agreement becomes worse since the SF model fully accounts for tails, in contrast to GSA.

One may wonder why there is a relatively high deviation in the few layers next to the surface layer. In these layers tail segments hardly contribute. The maximum difference (around 25 %) is found for $z' = 2$. The reason is the strong variation of $\phi(z)$ in this region, so that the continuum version of the second derivative $\ddot{g}_c \equiv d^2g/dz^2$ is not equal to the discrete version $\ddot{g}_d \equiv g(z-1) - 2g(z) + g(z+1)$. For the functional dependence $g(z) = (z + D)^{-1}$ it is easily shown that $\ddot{g}_d/\ddot{g}_c = (z+D)^2 / \{(z+D)^2 - 1\}$, which is close to unity for large z . However, for $z = 3/2$ ($z' = 2$) there is an appreciable difference, which leads to too low values of g and $\phi \sim g^2$ in the continuum model. For smaller values of χ_s (larger D), where g and ϕ vary more slowly with z , the ratio \ddot{g}_d/\ddot{g}_c is closer to unity and the agreement between the analytical and numerical models in the inner part of the profile is then better.

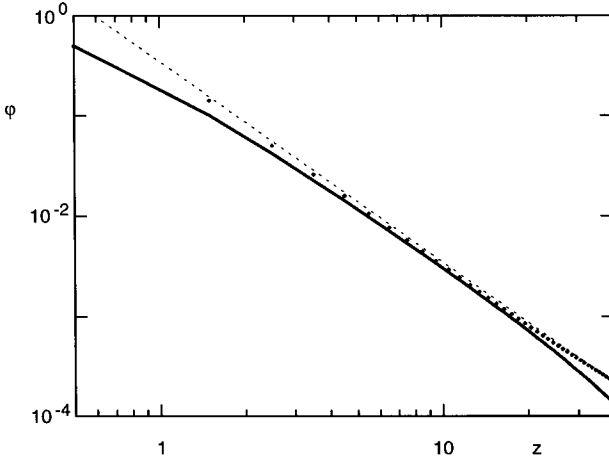


Fig. 4. As fig. 3, but now for $N = 10^5$ and $d = 34.5$. The dotted line with slope $\alpha = 2$ was drawn for comparison.

Another example for a higher chain length $N = 10^5$ is given in fig 4. In this case $d = 34.5$. The same trends are observed as in fig. 4; the main difference, obviously, is that the central region is wider. The slope of the double-logarithmic plot is quite close to the scaling exponent $\alpha = 2$ for this high chain length, as seen from the straight line drawn in the figure. In the following section, we analyse in some detail this exponent as a function of D and d .

The central power-law exponent

The mean-field power-law exponent is found as the slope $\alpha(z) = -d \log \phi / d \log z$ in the central region. If the scaling laws apply, it should be equal to 2, independent of z . This would imply a linear plot of $\log \phi$ against $\log z$. As can be seen in figs. 3 and 4, this is approximately correct but there are deviations, both for GSA and SF, which depend on N and ϕ^b (through d) and on χ_s (through D). In GSA it is easy to find an expression for $\alpha(z)$. From differentiation of eqs. 10 or 11b:

$$\alpha(z) = \frac{2z}{d} \coth \frac{z+D}{d} \approx 2 \left\{ \frac{z}{z+D} + \frac{z(z+D)}{3d^2} \right\} \quad (17a,b)$$

which shows the (weak) z -dependence explicitly. It is immediately clear that $\alpha(z) \rightarrow 2$ for $D \ll z$ and $d \rightarrow \infty$. In order to see how the exponent depends on D and d , we define the central region as the region between $z = 3$ and $z = d$, and take the slope halfway between these points, at $z = z_1$. The choice to start in layer 3 is to some extent arbitrary (and only acceptable when $D \ll 3$), but could be motivated by considering that layer $z' = 1$ definitely does not belong to the central region, and that for $z' = 2$ GSA is relatively inaccurate, as discussed above. In a linear plot the normal choice for z_1 would be $z_1 = (3 + d)/2$. Since in our case we derive the slope from a logarithmic plot, the natural choice is $\log z_1 = (\log 3 + \log d)/2$, or $z_1 = \sqrt{3d}$. Hence, we obtain a measure for the exponent in GSA by substituting $z = \sqrt{3d}$ in eq. 17. From eq. 17a:

$$\alpha = \frac{2\sqrt{3}}{\sqrt{d}} \coth \frac{D + \sqrt{3d}}{d} \quad (18)$$

which upon expansion in terms of $1/d$ gives the limiting behaviour

$$\alpha = 2 - \frac{2D}{\sqrt{3d}} + \frac{6 + 2D^2}{3d} \quad (19)$$

The same result is obtained from eq. 17b.

For small D , $\alpha \approx 2 + 2/d$, which gives a first-order estimate of the correction as a function of chain length and solution concentration. For relatively short chains this correction is significant. For example, for $N = 10^3$ and $\phi^b = 10^{-4}$ ($d \approx 4.6$) and $\chi_s = 1$ it would amount to 0.4 ($\alpha = 2.4$), but one has to realise that in this case the central region is almost absent, comprising just two lattice layers (segment lengths). For such short chains the proximal region crosses directly to the distal region, without a power-law region in between.

In fig. 5 we show how for longer chains (in this case $N = 10^4$) α depends on χ_s . The GSA exponent in this figure was obtained from eq. 18, the numerical SCF exponent from the numerical data. In the latter case α was calculated as $\alpha = \log[\phi(z_1 + 1)/\phi(z_1)] / \log[z_1/(z_1 + 1)]$, where z_1 is the integer closest to $\sqrt{3d}$. For high χ_s , α is above 2 because D is small and the last term of eq. 19 is much larger than the second. For increasing D (decreasing χ_s) the second term starts to contribute significantly and α becomes smaller, dropping below 2 for $\chi_s < 0.5$. For even smaller χ_s the average slope decreases rather strongly, but in this case log-log plots as

given in figs. 3 and 4 become more and more rounded, which makes a central region with a constant power-law exponent questionable. At any rate, it is gratifying that there is good agreement between GSA and the numerical results in fig. 5.

We note that Van der Linden en Leermakers obtained higher corrections for the same SF data. The reason is that they plotted $\log \phi$ against $\log z'$, and not against $\log z$, which is more appropriate. The difference may not seem large, but it is significant if α is to be obtained from a small region where z is small, as is the case for short chains.

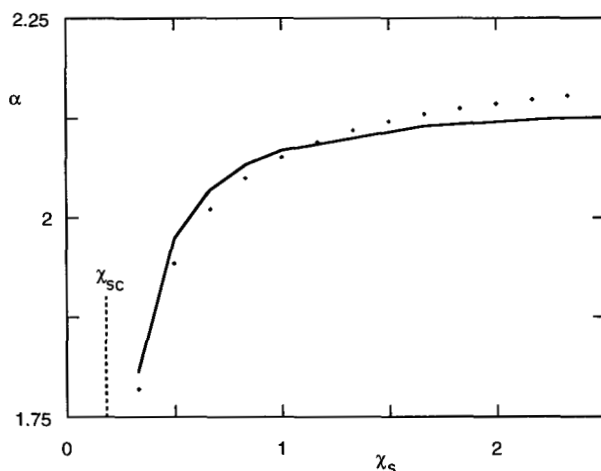


Fig. 5. The slope α of the double-logarithmic plot of ϕ against z in the central region (evaluated at $z = \sqrt{3d}$) according to the numerical SCF model (data points) and GSA (eq. 18) as a function of χ_s , for $N = 10^4$ and $\phi^b = 10^{-7}$.

Poor solvents

We do not give detailed results in this paper for poor solvents, but point out some implications of the above analysis for $\chi = 0.5$ (theta solvent). In this case the linear term in the expansion of $u \approx -\ln(1-\phi) - 2\chi\phi$ vanishes, and $u \approx (1/2)\phi^2 = (1/2)g^4$. Now the ground-state differential equation reads $(1/6)d^2g/dz^2 = (g^4/2 + \epsilon)g$ instead of eq. 7, and the solution for $\phi = g^2$ is

$$\phi = \frac{1}{d} \operatorname{csch}\left(\frac{2(z+D)}{d}\right) \approx \frac{1}{2(z+D)} \exp\left(-\frac{2(z+D)^2}{3d^2}\right) \quad (20a,b)$$

which may be compared with eqs. 10 and 11b, respectively. The scaling in the central region is $\varphi \propto z^{-1}$, as expected, but the d -dependent correction is stronger in this case. This is also borne out by taking the derivative $\alpha = -d \ln \varphi / d \ln z$:

$$\alpha(z) = \frac{2z}{d} \coth\left(\frac{2(z+D)}{d}\right) \approx \frac{z}{(z+D)} + \frac{4z(z+D)}{3d^2} \quad (21a,b)$$

which may be compared with eq. 17. If we again take the slope at $z = \sqrt{3d}$ as the criterion for the power law-exponent, we find the analogon of eqs. 18 and 19:

$$\alpha = \frac{2\sqrt{3}}{d} \coth\left(\frac{2(D+\sqrt{3d})}{d}\right) \approx 1 - \frac{D}{\sqrt{3d}} + \frac{4+D^2/3}{d} \quad (22a,b)$$

which shows that for high χ_s (low D) α is given by $\alpha = 1 + 4/d$, which makes the correction for finite chain lengths relatively more important than in good solvents. In this case eq. 13 also has a different form, which we do not give here; we note only that the strong adsorption limit for D is given by $\varphi(1/2) = (1/2)(D+1/2)^{-1} = 1$, or $D = 0$.

Discussion

In this paper we have shown that also in a mean-field picture the polymer adsorption profile splits up into proximal, central and distal parts as suggested by De Gennes. Using a ground-state approximation we were able to derive how the proximal length D depends on the adsorption energy. The distal length d depends in first approximation only on the chain length and on the polymer concentration in the bulk solution: $d \approx R_g / \sqrt{\ln(1/\varphi^b)}$. In experimentally accessible conditions the chain length is finite ($N \approx 10^5$ may be an upper limit as it corresponds to a molar mass of order 10^7), the bulk concentration is often in the dilute regime (ppm range or below), and the adsorption energy is usually of the order of kT . In this case the difference between D and d is not large enough to guarantee perfect universal scaling in the central regime, which is expected for $D \ll z \ll d$. The scaling exponent (evaluated at $\sqrt{3d}$) is shown to be $\alpha \approx 2 + 2d^{-1}$, and can be significantly above 2, especially for relatively short chains and low solution concentrations; the central region is then quite narrow. The deviation from the scaling result $\alpha = 2$ is attributed to the fact that in experimentally relevant conditions one is likely to obtain a value affected by the finite size of central region. We thus expect a cross-over behaviour wherein the chain length and polymer concentration remain important.

In poor solvents the deviations from the universal scaling exponent ($\alpha = 1$ in this case) are even larger so that it would be rather unlikely that the scaling $\varphi \propto z^{-1}$ could be observed experimentally for real systems.

For excluded-volume blobs the scaling exponent in the central region is $4/3$ as discussed by De Gennes. This exponent is significantly smaller than the value 2 found in the mean-field treatment. Because of the higher exponent, the central part of the profile extends further into the solution because R now scales as $N^{3/5}$. For example, for $N = 10^5$ the upper boundary shifts with a factor of about 3 because $N^{3/5} \approx 3N^{1/2}$ for

this value of N . The central region for this chain length would then be about 1.5 decade wide on a log-log plot (at $\phi^b = 10^{-7}$), as compared to one decade for mean-field scaling. However, the central region is now smaller near the surface because here we expect a cross-over from the concentrated to the semi-dilute regime. It is possible to avoid this cross-over by choosing a system with a low adsorption energy. However, a low adsorption strength causes the proximal length D to increase significantly. As we have seen, this in turn will make the central region narrower. Hence, it is difficult to avoid that the (universal) excluded-volume scaling starts further out from the surface as compared to the self-similar scaling in the mean-field treatment. If this shift is only a few layers, on a logarithmic plot a considerable part of the gain at the outside of the profile is lost. Thus, we expect difficulties for finding a wide central regime in experimental systems. Probably, the cross-over corrections as discussed in the context of the mean-field treatment will more generally play a role. So far, only very few experiments are reported wherein the excluded-volume scaling is found. We believe that more experiments are needed to establish the scaling behaviour in the central part of the polymer adsorption profile. On the basis of our analysis one would expect a non-universal "averaged" scaling in the central region which, however, again follows well-defined rules. Carefully designed experiments with finite (but not too small) chain lengths and low polymer concentrations would be needed to investigate our conjecture. The extrapolation of our findings to systems with excluded-volume correlations may also be investigated by computational techniques. Work in this area is currently underway in our laboratory.

Conclusions

There is a correction to the scaling exponent in the self-similar density profile of adsorbed polymers for most experimentally accessible conditions. This correction is proportional to $\sqrt{\ln(1/\phi^b)}$ and inversely proportional to \sqrt{N} , and originates from the fact that under most conditions the central regime is not very wide and is modified by cross-over effects. In the literature it was already recognised that the proximal length D generally modifies the self-similar behaviour, especially for small distances from the surface (when the adsorption strength is not too high). In this paper we show that the distal length d also effects the (measurable) power-law behaviour in the central part of the density profile. These crossing-over phenomena have the effect that the density profiles are less universal than usually is assumed.

In the GSA approximations expressions for the two relevant lengths d and D can be derived without the need to fit the profile to exact numerical data. This enables full analytical evaluation of the density profile (and other properties like adsorption isotherms) within the GSA scheme. Including tails in the analysis is possible as shown recently by Johnner et. al. [7]. The effects of tails on the scaling as discussed in the present paper are not very large, as indicated by the fact that the GSA results are in good agreement with numerical self-consistent-field calculations wherein tails are explicitly accounted for.

We anticipate that the mean-field results can be extrapolated to real systems. Our arguments for this are that on a log-scale the size of the central regime in a system with excluded-volume correlations is probably not much larger than in a mean-field system.

References

1. Fler GJ, Scheutjens JM, Cohen Stuart MA, Cosgrove T, Vincent B, *Polymers at Interfaces* (Chapman & Hall, London), 1993.
2. De Gennes PG: *Macromolecules* 1981, **14**: 1637.
3. Van der Linden CC, Leermakers FAM: *Macromolecules* 1992, **25**: 3449.
4. Scheutjens JM, Fler GJ: *J Phys Chem* 1979, **83**: 1619.
5. Scheutjens JM, Fler GJ: *J Phys Chem* 1980, **84**: 178.
6. Ploehn HJ, Russel WB, Hall CK: *Macromolecules* 1988, **21**: 1075.
7. Johnner A, Bonet-Avalos J, Van der Linden CC, Semenov AN, Joanny JF: *Macromolecules* 1996, **29**: 3629.
8. Joanny JF, Johnner A: *J de Physique II* 1996, **6**: 511.
9. Fler GJ: Symposium "Molecular order and mobility in polymer systems", St Petersburg (1996); *Macromolecular Symposia* 1997, **113**: in press. This paper gives a slightly different version of eq. 13 in the present paper.
10. Scheutjens JM, Fler GJ, Cohen Stuart MA: *Colloids Surfaces* 1986, **21**: 285.
11. Hong KM, Noolandi J: *Macromolecules* 1981, **14**: 727.
12. Edwards SF: *Proc Phys Soc* 1965, **85**: 613.